eISSN: 09748369, www.biolmedonline.com

Real-time OCT for study of cornea of living Indian frogs and toads

Kumari S*, Nirala AK
Biomedical Optics Laboratory, Department of Applied Physics, Indian School of Mines, Dhanbad, Jharkhand-826004 (India).

***Corresponding Author:** sule_baij@yahoo.co.in

Abstract
A high-speed Optical Coherence Tomography (OCT) system based on single mode fiber which can capture eight images per second was used to acquire OCT images of the eyes of Indian frogs and toads. The axial resolution of the set up was estimated to be 18 μm. With these OCT images, the ocular parameters, viz. corneal thickness, anterior chamber depth and anterior chamber angle were estimated. The thickness of the cornea of frog and toad is found to be 136.12 μm and 100.66 μm respectively. Measurement of corneal thickness is needed in many physiological and clinical studies and is helpful in diagnosis of several corneal disorders.

Keywords: Optical coherence tomography; Cornea; Indian Frog; Toad.

Introduction

Optical Coherence Tomography (OCT) is a relatively new noninvasive, noncontact, promising, imaging technique which gives high resolution cross-sectional images from beneath the surface of the skin, into the eye, or used for images of other tissues (Bouma and Tearney, 2002; Huang et al.,1991). The most familiar clinical tomographic imaging techniques known today are X-ray, computed tomography (CT) imaging, magnetic resonance imaging (MRI) and ultrasound. OCT's uniqueness results from its unsurpassed imaging resolution of 1-20 μm whereas typical clinical resolutions of MRI and ultrasonography are of the order of 1mm and 200μm respectively.

Measurement of corneal thickness is needed in many physiological and clinical studies and is helpful in diagnosis of several corneal disorders. The fine structure of frog cornea has been studied using histological technique and compared with that of the rabbit cornea, particularly in relation to the uptake and transport of colloidal particles (Kaye et al., 1962). An optical interferometry method was developed for measuring the thickness of cornea in frog (normal bullfrog - *Rana catesbeiana*) and human cornea (Green et al., 1975). In this method, the image information is limited to one dimension. A high-speed optical coherence domain reflectometer was described for measuring the distances of anterior eye structures in an anesthetized Dutch pigmented rabbit in vivo (Swanson et al., 1992). Using light source of low coherence length and the Doppler principle, thickness of human cornea in vivo was measured (Hitzenberger et al., 1992). This method is limited for one-dimensional measurement. The application of OCT system, which is interfaced with a slit lamp bimicroscope, was demonstrated to perform imaging studies in the anterior eye in vivo (Izatt et al., 1994). The technique of full-field OCT which uses a white light source was used for ocular tissue imaging (Griev et al., 2004). Using this technique unstained tissue samples of rat, mouse and pig under immersion was examined.

A high-speed, ultrahigh-resolution, 3-dimensional optical coherence tomography (3D OCT) was demonstrated for retinal imaging (Wojtkowski et al., 2005). Several ocular parameters, viz. corneal thickness, mean retinal thickness and effective refractive index, gradient refractive index profile of crystalline lens of zebra fish eye was estimated, using OCT (Rao et al., 2006; Verma et al., 2007). In situ imaging of retinal layers and surrounding ocular tissues using time-domain common-path optical coherence tomography was investigated (Han et al., 2010). In order to increase the accuracy and reduce noise we used real-time OCT. OCT is currently the most precise technique for the measurement of corneal thickness in vivo. In the cornea, OCT could become a useful tool in guiding highly precise keratorefractive surgeries.

In this paper, we report (first time to the best of our knowledge) the results of experiments using high-speed real-time OCT techniques for the measurement of the thickness of cornea, anterior chamber depth and angle of

anterior chamber of the eyes of Indian frog and toad in vivo. Corneal thickness is also useful in diagnosis and management of problems related to corneal edema etc. In these amphibians, an important parameter is affected by environmental stress and infection. The anterior chamber angle is very important structure in the eye. A narrow angle increases the risk of acute angle glaucoma.

We chose Indian frog (*Rana tigrina*), scientific name - *Hoplobatrachus tigerinus*, as a sample because the anatomy of frog is very similar to the anatomy of man. The frog's anatomy, however, is much simpler. The cornea of the normal adult frog closely resembles with that of other higher vertebrates. Due to the fact of total absence of terminal bars or heptameters in the endothelium of the frog cornea, as well as the complex interleaving of the lateral margins of the endothelial cells of the frog cornea, this layer in frogs most nearly resembles that in the human. The other sample we chose was Indian toad whose scientific name is *Bufo melanostictus* of family Bufonidae.

Amphibia is the base line for the study of human beings. Every work is the outcome of the amphibian study. Hence, the present work is significant for the study of eyes. Further study will be easily done by putting chemicals on the eye of frog.

Theory of OCT

OCT is an extension of low coherence reflectometry (Huang et al., 1991) where the sample is scanned in a transverse dimension to produce a profile of backscatter versus depth in a two-dimensional thin slice of tissue. The central part is Michelson interferometer illuminated by low coherence light source. One arm of the interferometer is replaced by the sample under investigation. The reference mirror is scanned with constant speed v_r, to produce interference modulation with Doppler frequency $f = 2v_r/\lambda$, where λ is the mean wavelength of the source. Then the interference can occur at detector only when the path difference between these two waves is less than the coherence length of light. Scanning the reference arm path length provides depth resolved information. A source of low coherence light is used to provide high axial resolution and is given by

$$\Delta z = \left(\frac{2\ln 2}{\pi}\right)\left(\frac{\lambda^2}{\Delta\lambda}\right)$$

where Δz is the axial resolution, λ is the mean wavelength and $\Delta\lambda$ is the spectral width.

The basic measurement performed in OCT imaging is an interferometric cross-correlation of light returning from the reference and sample arms as a function of the optical path length difference Δl between the arms.

Frogs and Toads

Frogs and toads are tail-less amphibians. Frogs generally have protruding eyes, narrow body and waist, strong, long and webbed hind feet adapted for leaping and swimming, and smooth, moist skin. They generally have no warts on their body. Toads have a squat body (broad, flat body), warts on body, rough, dry skin, short legs and teeth in upper jaw. There are more than 300 species of true toads (family Bufonidae) which are found almost worldwide. They have thick, dry, often warty skin. Frogs generally live near or in water while toads live on land but breed in water only. Compared to frogs, toads have a more complex and versatile visual system due to their more general eating behavior.

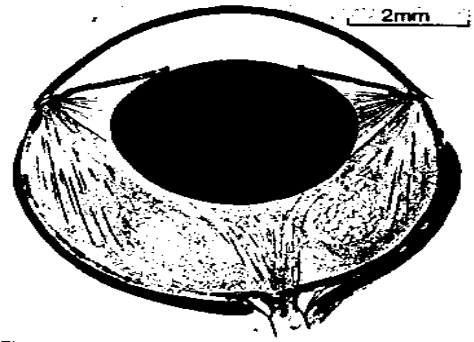

Fig. 1 - Eye of the frog.

The eye of frog is crude. Its fixed lens cannot change its focus. Poorly developed eyelids do not move. To close its eye, the frog draws the organ into its socket. A Frog hunts on land by vision. Frogs will starve to death surrounded by food if it is not moving. Frog has no fovea or region of greatest acuity in vision upon which it must centre a part of the image. It has only a single visual system, retina to colliculus, not a double such as ours.

The large round lens of the frog gives it a large field of view. The frog is naturally nearsighted to 6 diopters giving it a focus of approximately 6 inches. Frogs and toads can change their focus by moving the lens out towards the cornea. In frogs, the focus range is a few diopters and in toads, the focus range is 5 diopters giving a best myopia of 1 diopter. The advantage of nearsightedness is that it blurs the background clutter making foreground object characterization much easier.

The cornea of *Rana pipiens* measures approximately 100 microns. The cornea of *Rana catesbeiana* is approximately twice this thickness. The epithelium and stroma of the frog and toad cornea is similar to that of most mammalian corneas (Kaye, 1962).

Materials and Methods

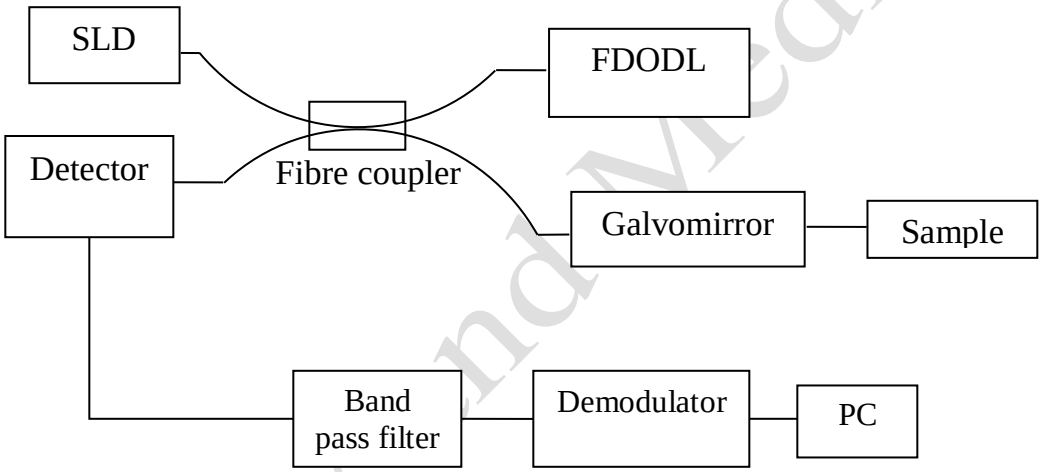

Fig. 2 - Schematic diagram of real-time OCT set-up.

Because OCT images are characterized by very high spatial resolution, even slight movements of the sample with respect to the probe beam during image acquisition can introduce significant motion artifact, the most straightforward and effective way to mitigate the problem is simply acquire images quickly with respect to the time scale of the motion. Because of motion artifact as well as issue of ease- of-use and the need to minimize procedure time, practical OCT imaging is best performed in real-time. The real-time OCT system used to acquire the images rapidly is a fiber optic based Michelson interferometer as shown in fig. 2. The system utilizes a high power broadband source and real-time image acquisition hardware and features a high-speed scanning delay line in the reference arm based on Fourier-transform pulse shaping technology (Rollins et al., 1998). A high-speed scanning optical delay line in the reference arm of the OCT system is included in order to acquire images rapidly. The imaging speed of the set up was eight frames per second. Scanning range was 0 to 3 mm. Superluminescent diode (SLD) of wavelength 1310 nm with bandwidth 30 nm was used as a light source. In this wavelength region, the transmittance of ocular medium is reduced. The other advantage of using illumination at this longer wavelength is that the amount of scattering is less. We used high-speed OCT to examine anterior segment parameters, such as corneal thickness, central anterior chamber depth and angle of anterior chamber. Use of

1310 nm illumination for anterior segment OCT allows for increased penetration in scattering tissues such as the sclera and iris, while simultaneously permitting sufficient illumination power to be used to enable high-speed imaging. The light from SLD passes through the two-port fiber coupler. The fiber coupler splits the light into two parts: one towards reference arm and other towards sample arm. There is high-speed scanning delay line in the reference arm which is also known as Fourier domain optical delay line. In this delay line a flat mirror serves as a spatial phase filter, which imposes a linear phase ramp in the frequency domain.

An AGC driver (electro-optical products corporation make) was used for scanning the reference arm. The driver was connected to logarithmic amplifier and CPU of computer through the connectors, line synchronization. The logarithmic amplifier is connected to the LP/HP/BP/BR Butterworth/Bassel multichannel filter (Krohn-Hite Corp. make). The light coming from the sample and reference arm is combined at the detector. The images were acquired using high-speed PC. The driver is used to rotate the galvoscanner mirror in order to produce Doppler frequency to get the result in shot noise limited region (Rao et al., 2006).

Procedure

Sample was taken as a frog of length 4.50 cm (snout to anus) and width 2.5 cm (measurement taken from dorsal side). Frog was anaesthetized using chloroform kept in petridish. Then, the petridish was kept in the set-up for imaging and images of the frog's eye were taken. The light incident on frog's eye is ensured to be perpendicular. The real-time OCT images that are given below are the representative figures which we found during experiments. Fig. 3 & 4 show the real-time OCT images of the eye of the living frog. In this figure of cornea, anterior portion of crystalline lens and iris is clearly visible.

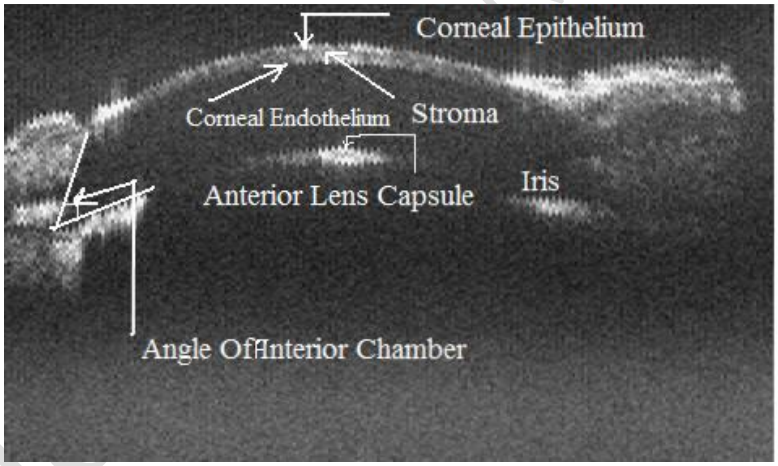

Fig. 3 - Real-time OCT image of anterior segment of frog's eye (in vivo).

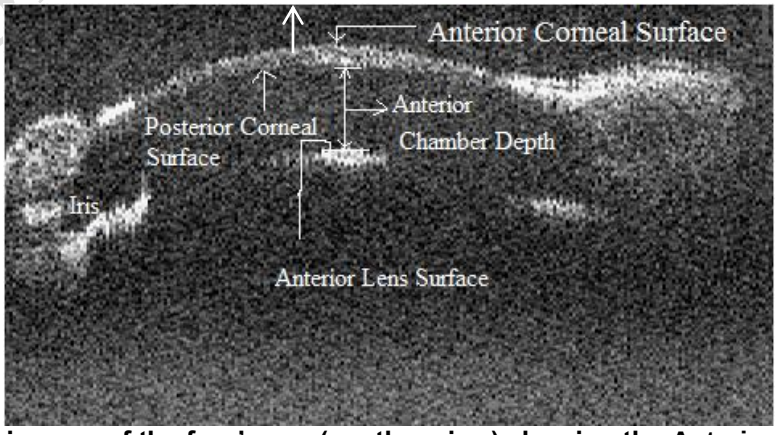

Fig. 4 - OCT images of the frog's eye (another view) showing the Anterior Chamber Depth.

Another sample was taken as a toad of length 4.5 cm (snout to anus) and width 3.2 cm (measured from dorsal side) which was anesthetized using the chloroform. The toad lost physical movement within 2-3 minutes and the petridish was kept in the set-up for imaging. Fig. 5 & 6 show the real-time OCT images of the eye of toad. Due to poor resolution in this figure only cornea, iris and anterior portion of crystalline lens is visible. It is assumed that in the case of toad the image is not of good contrast due to non-protruding eyes. Therefore, average of eight images was taken in order to reduce the noise (fig. 7). The image pixel size is 480 x 312 pixels and the size of the image is 4mm x 4mm.

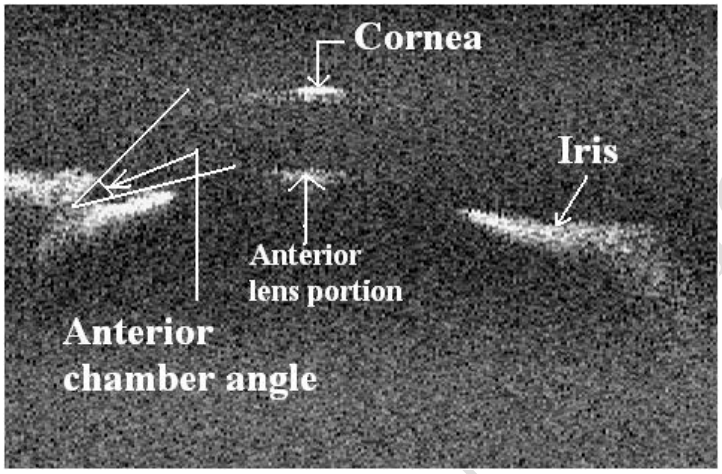

Fig. 5 - Real-time OCT image of toad's eye (in vivo).

Fig. 6 - OCT images of the toad's eye (another view).

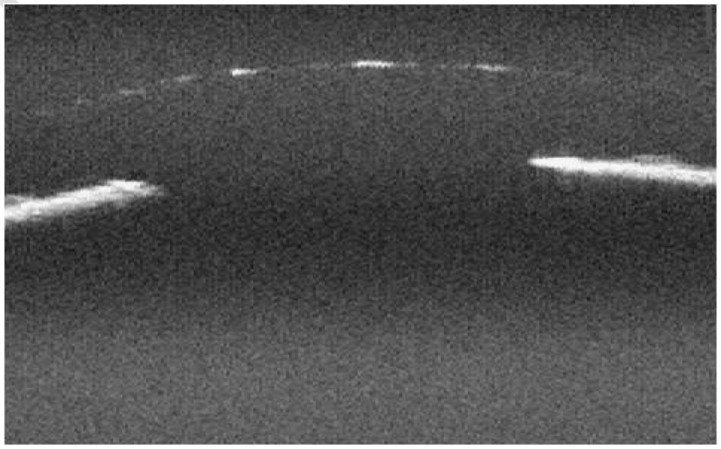

Fig. 7 - Average of eight images of toad's eye.

Results and Discussion

The optical path through the cornea is taken as the distance between the endothelial and epithelial maxima. The geometric thickness of the cornea equals the optical pathlength divided by the group refractive index of the cornea, which was assumed 1.35. Measurements were performed in the center of the cornea. The system is capable of differentiating three corneal layers. The highest reflectivity is found at the epithelium of Bowman layer and at the discemet endothelial layer; whereas lower reflectivity is observed in the corneal stroma. The geometrical thickness of cornea of frog (central corneal thickness), in the region where the OCT light is perpendicular to the cornea, turned out to be approximately 136.12 μm. The maximum corneal thickness obtained for frog is 151.94 μm and that of minimum thickness is 113.96 μm. For toad, central corneal thickness is found to be 100.66 μm. The values of corneal thickness obtained were compared with standard value obtained (Green et al., 1975; Kaye, 1962) and found to be of the same order. It should be noted that since the resolution of the set-up is ~ 17.78 μm, we could not resolve the epithelium layer of the cornea, in spite of the fact that we carried a large number of experiments. The measured value of average anterior chamber depth of the frog's eye is 465.33 μm while the average anterior chamber depth of toad eye is 417.85 μm. In addition, the average angle of anterior chamber the frog's eye is 42 ° and that of the toad eye is 37°.

Conclusion

Experimentally measured optical and geometrical thickness of the cornea of Indian frog's eye was 183.76μm. and 136.12 μm respectively. In case of Indian toad's eye, the corneal optical thickness was experimentally found to be 135.89 μm and that of geometrical thickness was equal to 100.66 μm. The images in the case of frog are of good quality while in the case of toad it is not so. The reason may be due to the bulging eyes of frog.

Acknowledgement

We sincerely acknowledge the financial assistance given by DST, New Delhi as sponsored project no. "SR/S2/LOP-07/2005 dated 24/10/2007" without which it would not have been possible to perform this work. We are also thankful to Professor P.K. Gupta and his group at RRCAT, Indore for their help and cooperation in conducting the experimental work.

References

Bouma BE, Tearney GJ, 2002. Handbook of Optical Coherence Tomography. Dekker, New York.

Green DG, Frueh BR, Shapario JM, 1975. Corneal thickness measured by interferometry. Journal of the Optical Society of America, 65: 119-123.

Grieve K, Paques M, Dubois A, Sahel J, Boccara C, Gargasson J, 2004. Ocular tissue imaging using ultrahigh-resolution full-field optical coherence tomography. Investigative Ophthalmology and Visual Science, 45: 4126-4131.

Han JH, Ilev IK, Kim DH, Song CG, Kang JU, 2010. Investigation of gold-coated bare fiber probe for in situ intra-vitreous coherence domain optical imaging and sensing, Applied Physics B: Lasers and Optics, 99: 741-746.

Hitzenberger CK, 1992. Measurement of corneal thickness by low coherence Interferometry. Applied Optics, 31: 6637- 6642.

Huang D, Swanson EA, Lin CP, Schuman JS, Stinson WG, Chang W, Hee MR, Flotire T, Gregory K, Puliafito CA, Fujimoto G, 1991. Optical coherence tomography. Science, 254: 1178-1181.

Izatt JA, Hee MR, Swanson EA, Lin CP, Huang D, Schuman JS, Puliafito CA, Fujimoto JG, 1994. Micrometer-scale resolution imaging of the anterior eye *in vivo* with optical coherence tomography. Archives of Ophthalmology, 112: 1584-1589.

Kaye GI, 1962. Studies on the cornea III. The fine structure of the frog cornea and the uptake and transport of colloidal particles by the cornea in vivo. The Journal of Cell Biology, 15: 241-258.

Rao D, Verma Y, Gupta PK, 2006. Optical coherence tomography. Kiran, 17: 69-74.

Rollins AM, Kulkarni MD, Yazdanfar S, Ung-arunyawee R, Izatt JA, 1998. In vivo video rate optical coherence tomography, Optics Express, 3: 219-229.

Rao KD, Verma Y, Patel HS, Gupta PK, 2006. Non-invasive ophthalmic imaging of adult zebrafish eye using optical coherence tomography, Current Science, 90: 1506-1510.

Swanson EA, Huang D, Hee MR, Fujimoto JG, Lin CP, Puliafito CA, 1992. High-speed optical coherence domain reflectometry. Optics Letters, 17(2): 151-3.

Verma Y, Rao KD, Suresh MK, Patel HS, Gupta PK, 2007. Measurement of gradient refractive index profile of crystalline lens of fisheye in vivo using optical coherence tomography. Applied Physics B: Lasers and Optics, 87(4): 607-610.

Wojtkowski M, Srinivasan V, Fujimoto JG, Ko T, Schuman JS, Kowalczyk A, Duker JS, 2005. Three-dimensional retinal imaging with high-speed ultrahigh-resolution optical coherence tomography. Ophthalmology, 112(10): 1734-1746.